

# THE GEOMETRY EFFECTS OF AN EXPANDING UNIVERSE ON THE DETECTION OF COOL NEUTRAL GAS AT HIGH REDSHIFT

S. J. CURRAN

Sydney Institute for Astronomy, School of Physics, The University of Sydney, NSW 2006, Australia and  
 ARC Centre of Excellence for All-sky Astrophysics (CAASTRO)

*Draft version August 22, 2018*

## ABSTRACT

Recent high redshift surveys for 21-cm absorption in damped Lyman- $\alpha$  absorption systems (DLAs) take the number of published searches at  $z_{\text{abs}} > 2$  to 25, the same number as at  $z_{\text{abs}} < 2$ , although the detection rate at high redshift remains significantly lower (20% cf. 60%). Using the known properties of the DLAs to estimate the unknown profile widths of the 21-cm non-detections and including the limits via a survival analysis, we show that the mean spin temperature/covering factor degeneracy at high redshift is, on average, double that of the low redshift sample. This value is significantly lower than the previous factor of eight for the spin temperatures and is about the same factor as in the angular diameter distance ratios between the low and high redshift samples. That is, without the need for the several pivotal assumptions, which lead to an evolution in the spin temperature, we show that the observed distribution of 21-cm detections in DLAs can be accounted for by the geometry effects of an expanding Universe. That is, as yet there is no evidence of the spin temperature of gas rich galaxies evolving with redshift.

*Subject headings:* quasars: absorption lines — radio lines: galaxies — galaxies: star formation — galaxies: evolution — galaxies: ISM — cosmology: observations

## 1. INTRODUCTION

The 21-cm transition of hydrogen (H I) traces the cool component of neutral gas throughout the Universe, the raw material fuelling star formation. In emission, the low probability of the 21-cm spin-flip transition compounded by the inverse square law, renders this essentially undetectable at  $z \gtrsim 0.2$ . In absorption, however, this sensitivity limit can be avoided since the line strength is independent of distance, depending only upon the column density of the absorbing gas and the flux from the background emission source. Nevertheless, detections remain rare with only 77 H I 21-cm absorption systems known at  $z \gtrsim 0.1$  — 35 associated with the quasar host galaxy ( $z_{\text{abs}} = z_{\text{QSO}}$ )<sup>1</sup>, in addition to 42 systems located at some intermediate redshift along the sight-line to the quasar ( $z_{\text{abs}} < z_{\text{QSO}}$ )<sup>2</sup>. These *intervening* absorbers occur in known or candidate<sup>3</sup> damped Lyman- $\alpha$  absorption systems (DLAs, defined by their large neutral hydrogen column densities,  $N_{\text{HI}} \geq 2 \times 10^{20} \text{ cm}^{-2}$ ). Currently there are 1500 DLAs known (Curran et al. 2002; Noterdaeme et al. 2009), which could contain over 80% of the neutral gas mass density of the Universe (Prochaska et al. 2005).

The velocity integrated optical depth of the 21-cm absorption,  $\tau \equiv -\ln\left(1 - \frac{\sigma}{fS}\right)$ , is related to the total neutral hydrogen column density via (Wolfe & Burbidge

1975)

$$N_{\text{HI}} = 1.823 \times 10^{18} T_{\text{spin}} \int \tau dv, \quad (1)$$

where  $T_{\text{spin}}$  [K] is the mean harmonic spin temperature of the gas,  $\sigma$  is the depth of the line (or r.m.s. noise in the case of a non-detection) and  $S$  &  $f$  the flux density and covering factor of the background continuum source, respectively. This latter parameter accounts for the possibility that the absorbing gas may not fully cover all of the background radio emission<sup>4</sup> and so all of the measured flux,  $S$ , may not be intercepted, decreasing the sensitivity of the observation.

In both the associated and intervening cases the detections occur overwhelmingly at  $z \lesssim 1$ . For the associated systems,  $N_{\text{HI}}$  is generally not known, although Curran et al. (2008) attribute the lack of absorption at high redshift to the traditional optical selection of targets biasing searches towards the most luminous objects at these large distances, where the ultra-violet luminosity ionises the neutral gas.

In the optically thin regime ( $\sigma \ll fS$ )<sup>5</sup> Equ. 1 reduces to  $N_{\text{HI}} = 1.823 \times 10^{18} \frac{T_{\text{spin}}}{f} \int \frac{\sigma}{S} dv$ , thus giving a degeneracy in the spin temperature/covering factor ratio ( $T_{\text{spin}}/f$ ), for the DLAs where the column density is known. Therefore, since there is a mix of detections and non-detections in DLAs at  $z_{\text{abs}} \lesssim 2$ , whereas at  $z_{\text{abs}} \gtrsim 2$  H I 21-cm tends not to be detected, Kanekar & Chengalur (2003) suggest an evolution in the spin temperature of the gas, where this is exclusively high at high redshift. This has direct bearing on the rel-

Electronic address: sjc@physics.usyd.edu.au

<sup>1</sup> Summarised in Curran & Whiting (2010), with the addition of three new associated absorbers reported in Curran et al. (2011a,c).

<sup>2</sup> Summarised in Curran (2010), with the addition of those reported by Curran et al. (2011b); Srikanand et al. (2012).

<sup>3</sup> Usually in Mg II absorption systems at  $z_{\text{abs}} \lesssim 1.7$ , thus not being sufficiently redshifted to be detected in the optical band by ground-based telescopes.

<sup>4</sup> Optical spectra from QSOs come from continuum sources  $\lesssim 1$  pc in diameter, whereas radio sources can exceed  $\sim 100$  pc (see Wolfe et al. 2005).

<sup>5</sup> Which applies to all but one of the known 21-cm absorbers (Roberts et al. 1976).

ative proportions of the cold and warm neutral media (e.g. Kanekar & Chengalur 2003; Srianand et al. 2012) and thus the reservoir of raw material available for star formation in the early Universe.

However, the conclusion that the spin temperature evolves with redshift relies on the assumption of a covering factor for each DLA, and Curran et al. (2005) have shown that, if the degeneracy is left intact,  $T_{\text{spin}}/f$  is not the order of magnitude larger at  $z_{\text{abs}} \gtrsim 2$ , as suggested by the  $T_{\text{spin}}$  distribution of Kanekar & Chengalur (2003). Furthermore, Curran & Webb (2006) suggest that geometry effects introduced by an expanding Universe could contribute to the distribution, indicating that the covering factor may actually be the dominant parameter. Since then there have been further high redshift searches (Curran et al. 2010; Srianand et al. 2012)<sup>6</sup>. This takes the number of confirmed DLAs and sub-DLAs searched for 21-cm to 25 at  $z \geq 2$ , the same number as at  $z \leq 2$ , thus allowing us to adequately address the spin temperature versus covering factor issue.

## 2. NEW H I 21-CM ABSORPTION SEARCH RESULTS

Although there are now equal numbers of 21-cm searches above and below  $z_{\text{abs}} = 2$ , the detection rate at  $z_{\text{abs}} > 2$  remains considerably lower (5 out of 25) than for the lower redshift sample (14 out of 25). Since the velocity integrated optical depth of the 21-cm absorption, normalised by the total neutral hydrogen column density, is proportional to  $f/T_{\text{spin}}$  (Sect. 1), this suggests that either  $T_{\text{spin}}$  is generally higher at  $z_{\text{abs}} > 2$  or that  $f$  is generally lower, or a combination of both, elevating the ratio at high redshift,

In order to obtain limits to the line strengths for the non-detections we must assign a profile width to each absorber. This is usually assumed, but here we estimate the full-width half maximum (FWHM) of the profile from the 21-cm FWHM—Mg II 2796 Å equivalent width correlation for the detections, specifically  $\text{FWHM} [\text{km s}^{-1}] \approx 13 \times W_r^{\lambda 2796} [\text{Å}]$  (Curran et al. 2007b). Where the Mg II equivalent widths are not available (generally at  $z_{\text{abs}} \gtrsim 2.2$  where the transition is redshifted out of the optical band), we estimate the putative FWHM via the metallicity—Mg II equivalent width correlation (Murphy et al. 2007), specifically  $W_r^{\lambda 2796} \approx 2.0 [\text{M}/\text{H}] + 4.0$  (Curran et al. 2007b). When neither the Mg II equivalent width nor metallicity are available, we assign a FWHM of  $25 \text{ km s}^{-1}$ , the mean of the detections.<sup>7</sup>

Given the FWHM of the putative line, in order to obtain the best signal-to-noise ratio, based upon the detection of a single channel we would smooth the data to a spectral resolution of  $\Delta v = \text{FWHM}$ . This has the effect of improving/degrading the measured r.m.s noise, and thus the optical depth, by a factor of  $\sqrt{\Delta v/\text{FWHM}}$ . The newly derived integrated optical depth of the line is thus

$$\left[ \int \tau dv \right]_{\text{new}} \approx \tau_{\text{peak}} \times \sqrt{\frac{\Delta v}{\text{FWHM}}} \times \text{FWHM}$$

<sup>6</sup> From the Sloan Digital Sky Survey DLA Data Releases 1–3 (Prochaska et al. 2005) and the SDSS DR7 DLA Data Release 7 (Prochaska et al. 2009), respectively.

<sup>7</sup> Excluding the FWHM =  $240 \text{ km s}^{-1}$  outlier due to the absorber in the complex sight-line towards 3C 336 (Curran et al. 2007a).

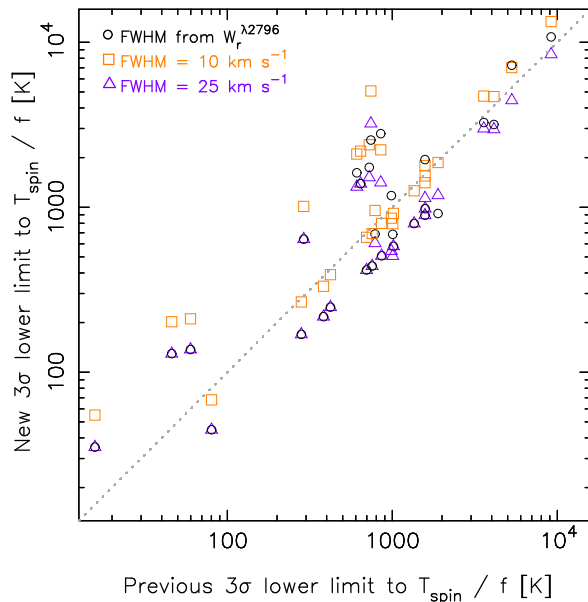


FIG. 1.— The lower limits to the spin temperature/covering factor degeneracy obtained from the recalculated velocity integrated optical depths versus those obtained from the previously published values. The circles show the values obtained by estimating the FWHM from the Mg II equivalent width, the squares using a FWHM of  $10 \text{ km s}^{-1}$  and the triangles using the mean  $25 \text{ km s}^{-1}$  of the detections. This is the default FWHM used when the Mg II equivalent width or metallicity is not available, thus giving the overlap between circles and triangles. The dotted line shows where the new and previous values are equal.

$$= \tau_{\text{peak}} \times \sqrt{\Delta v \text{ FWHM}}, \quad (2)$$

where  $\tau_{\text{peak}}$  is the peak optical depth of the putative line. This has the overall effect of scaling the previously published integrated optical depths, where these are calculated per channel, by  $[\int \tau dv]_{\text{new}} / [\int \tau dv]_{\text{previous}}$

$$= \frac{\tau_{\text{peak}} \times \sqrt{\Delta v \text{ FWHM}}}{\tau_{\text{peak}} \times \Delta v} = \sqrt{\frac{\text{FWHM}}{\Delta v}}. \quad (3)$$

We therefore recalculate the limits from the published r.m.s. noise levels and spectral resolutions and in Fig. 1 show the effect this has on the  $T_{\text{spin}}/f$  limits compared to the previous values. For the method prescribed above (shown as circles), the largest change is for the  $z_{\text{abs}} = 0.5579$  absorber towards PKS 0118–272, for which the limit climbs from  $T_{\text{spin}}/f > 850 \text{ K}$  (Kanekar & Chengalur 2001) to  $> 1900 \text{ K}$  and, on average, the scaled values are  $160 \text{ K}$  “warmer” than those published. As seen from the figure, however, the new limits are mostly concentrated close the  $[\int \tau dv]_{\text{new}} = [\int \tau dv]_{\text{previous}}$  line, with equal numbers of points to either side.

Curran et al. (2007b) attribute the correlation between the velocity spreads of the 21-cm and Mg II profiles to the neutral and singly ionised gas being spatially coincident in 21-cm detected DLAs. However, given the possibility that much of the ionised magnesium could arise in warm photoionised gas, and is thus not tracing the same sight-line as the 21-cm, in Fig. 1 we also show the  $T_{\text{spin}}/f$  limits derived from assuming a single FWHM. For  $10 \text{ km s}^{-1}$  (e.g. Srianand et al. 2012), we find the largest difference to be  $4300 \text{ K}$ , with a mean rise of  $600 \text{ K}$  and

for  $25 \text{ km s}^{-1}$ , the largest difference is  $2500 \text{ K}$ , with a mean decrease of  $120 \text{ K}$ . Thus, scalings implementing the mean FWHM of the detections have less of an effect than using  $10 \text{ km s}^{-1}$ , although either method is preferable to the inhomogeneously calculated published values, since each is consistent in smoothing the data to the FWHM and thus calculating the limit per smoothed channel.

In Fig. 2 we show the newly derived limits against the absorption redshift. Applying a survival analysis to the  $3\sigma$  lower limits in  $T_{\text{spin}}/f$ , via the ASURV package (Isobe et al. 1986), we obtain mean values of  $\overline{\log_{10}(T_{\text{spin}}/f)}_{z < 2} = 3.25 \pm 0.15$  and  $\overline{\log_{10}(T_{\text{spin}}/f)}_{z > 2} = 3.56 \pm 0.17$ . That is, the mean value of  $T_{\text{spin}}/f$  at  $z_{\text{abs}} > 2$  is double that at  $z_{\text{abs}} < 2$  ( $3600 \text{ cf. } 1800 \text{ K}$ ). This is considerably less than the ratio of  $8.0$  between the two redshift regimes ( $8100 \text{ cf. } 1020 \text{ K}$ ) found by applying the survival analysis to the spin temperatures of Kanekar & Chengalur (2003). Since our recalculation of the limits has actually slightly increased the mean value of the spin temperature/covering factor degeneracy, we attribute this significant difference to the covering factor being left as a free parameter.

### 3. SPIN TEMPERATURE OR COVERING FACTOR

The addition of the new data, together with our treatment of the non-detections, indicates that a factor of only  $\approx 2$  in the spin temperature/covering factor ratio between the two redshift regimes need be accounted for. However, it remains unclear whether  $T_{\text{spin}}$  or  $f$  is the dominant factor.

There have been several attempts to quantify the covering factor through Very Long Baseline Array (VLBA) imaging of the background quasar, in which  $f$  is estimated as the ratio of the compact unresolved component's flux to the total radio flux (e.g. Briggs & Wolfe 1983; Kanekar et al. 2009; Srianand et al. 2012). From this, Kanekar et al. (2009) conclude that for the 21-cm searches,  $f \geq 0.4$  and hence low covering factors cannot explain the dearth of detections at high redshift. However, this method gives no information on the extent of the absorber nor on how effectively it covers the emission. Neither does it give information on the depth of the line when the extended continuum emission is resolved out.

So although an evolution in spin temperature with redshift is implied, this method invokes several crucial assumptions which could even lead to unphysical results (e.g. the  $\sim 0 \text{ pc}$  obtained for the extent of PKS 0405–331 at  $398 \text{ MHz}$ , Kanekar et al. 2009). On the other hand, due to the effects of an expanding Universe, objects at  $1 \lesssim z \lesssim 4$  are always close to a single angular diameter distance ( $\sim 1500 \text{ Mpc}$ ), irrespective of redshift (e.g. Hogg 1999). Beyond  $z \sim 1$ , the angular diameter distance *decreases* with increasing redshift, which will lead to a natural imbalance between the low and high- $z$  DLA samples. In the small angle approximation the covering factor can be defined as

$$f \equiv \frac{d_{\text{abs}}^2}{DA_{\text{DLA}}^2 \theta_{\text{QSO}}^2} = \left( \frac{d_{\text{abs}} DA_{\text{QSO}}}{d_{\text{QSO}} DA_{\text{DLA}}} \right)^2, \quad (4)$$

where  $\theta_{\text{QSO}}$  is the angle subtended by the background emission and  $d_{\text{abs}}$  and  $d_{\text{QSO}}$  the linear sizes of the cool absorbing gas and background 21-cm emission, respectively (Fig. 3). Since absorbers at  $z \gtrsim 1$  are always at

a similar angular diameter distance as the background quasar ( $DA_{\text{DLA}} \approx DA_{\text{QSO}}$ ), these will therefore, for a given system, always have a lower coverage than a counterpart with  $DA_{\text{DLA}} < DA_{\text{QSO}}$  (Curran & Webb 2006), an inequality which can only exist at  $z \lesssim 1$ .

In Fig. 4 we show the angular diameter distance ratio,  $DA_{\text{DLA}}/DA_{\text{QSO}}$ , versus the absorption redshift for the 21-cm searches. Note that this distribution is free from any assumptions (including our own with regard to the FWHMs of the non-detections). From this we see a mix of  $DA_{\text{DLA}}/DA_{\text{QSO}}$  at low redshift (the low values are due to  $z \lesssim 1$  DLAs towards much higher redshift quasars), whereas values at  $z \gtrsim 1$  are exclusively high. That is, a reproduction of the ‘‘spin temperature’’ distribution of Kanekar & Chengalur (2003). At least the pattern if not the magnitude, given that Kanekar & Chengalur (2003) suggest that the average spin temperature at  $z_{\text{abs}} > 2$  is eight times that at  $z_{\text{abs}} < 2$ , which is clearly not reproduced in Fig. 4.

Referring to Sect. 2, however, we only require  $T_{\text{spin}}/f$  at  $z_{\text{abs}} > 2$  to be about double that at  $z_{\text{abs}} < 2$  in order to account for the distribution. From Equ. 4, for a given absorber and emitter size,  $f \propto 1/(DA_{\text{DLA}}/DA_{\text{QSO}})^2$ , and we find mean values of  $\overline{(DA_{\text{DLA}}/DA_{\text{QSO}})^2}_{z < 2} = 0.68$  and  $\overline{(DA_{\text{DLA}}/DA_{\text{QSO}})^2}_{z > 2} = 1.06$ , a ratio of  $1.6$ . It is therefore apparent that the distribution in angular diameter distance ratios, and their effect on the covering factor, is close to that required to account for the observed  $T_{\text{spin}}/f$  distribution.

Updating the statistics with the new results, we find a binomial probability of  $5.52 \times 10^{-5}$  of obtaining at least 9 out of 11 detections at  $DA_{\text{abs}}/DA_{\text{QSO}} < 0.8$  and 29 out of 39 non-detections at  $DA_{\text{abs}}/DA_{\text{QSO}} > 0.8$ , by chance.<sup>8</sup> That is, a significance of  $4.03\sigma$ , lending weight to the argument that large angular diameter distance ratios are correlated with the non-detection of 21-cm absorption. Since there is no physical link between the spin temperature and angular diameter distance ratio, this suggests that, in the absence of any knowledge of the absorption cross-section in relation to the emitter extent, the covering factor plays a much more major rôle than the spin temperature in the detection of 21-cm absorption.

### 4. DISCUSSION AND SUMMARY

With the advent of 21-cm absorption searches in high redshift DLAs there has been much debate on whether an evolution in spin temperature or lower covering factors are responsible for the relatively low number of detections at  $z_{\text{abs}} > 2$ . New searches of SDSS DLAs, which occult the sight-lines to radio-loud quasars, take the number searched at these redshifts to the same as at  $z_{\text{abs}} < 2$ , giving much needed data with which to address this issue. By giving the 21-cm non-detections a more thorough analysis than in other studies, through estimating the FWHMs of the non-detected profiles from the observed optical properties and applying a survival analysis to the

<sup>8</sup>  $DA_{\text{abs}}/DA_{\text{QSO}} = 0.8$  is the cut used by Curran & Webb (2006) and, although arbitrary, this is the lowest ratio which gives an appreciable enough sample size in the lower bin. When a ratio of  $0.9$  is used there are 38 DLAs with  $DA_{\text{abs}}/DA_{\text{QSO}} > 0.9$  and 12 with  $DA_{\text{abs}}/DA_{\text{QSO}} < 0.9$ , which increases the significance of the correlation to  $4.31\sigma$ .

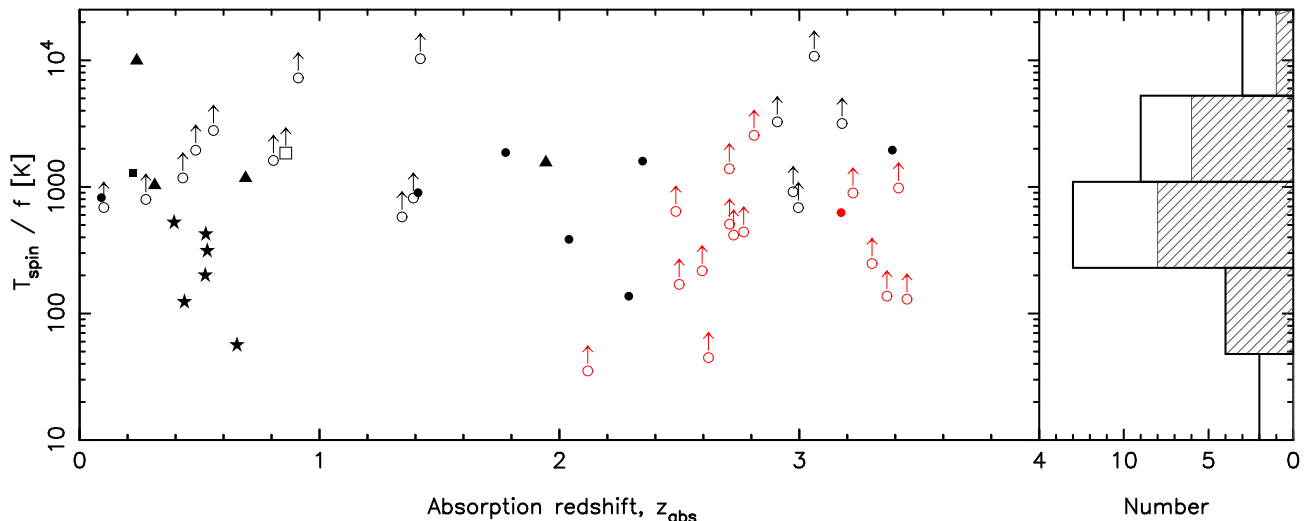


FIG. 2.— The spin temperature/covering factor degeneracy versus the absorption redshift for DLAs searched in 21-cm absorption. The filled symbols/histogram represent the detections, the unfilled symbols/histogram the non-detections ( $3\sigma$  limits), with the shapes representing the type of galaxy with which the DLA is associated: circle—unknown type, star—spiral, square—dwarf, triangle—low surface brightness (LSB). The coloured symbols show the recent high redshift searches of SDSS DLAs (Curran et al. 2010; Srianand et al. 2012). In the histogram the limits to  $T_{\text{spin}}/f$  are treated as actual values.

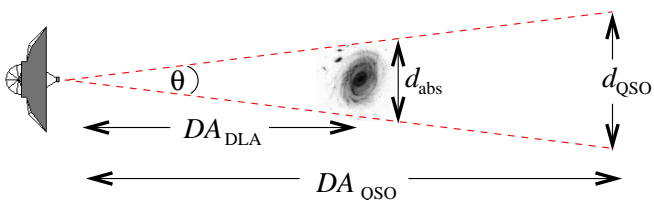


FIG. 3.— Absorber and quasar cross-sections with respect to the angular diameter distances. If the angle required to fully subtend  $d_{\text{abs}}$  is less than that to subtend  $d_{\text{QSO}}$  then  $f < 1$ .

lower limits in  $T_{\text{spin}}/f$ , we find:

1. That mean the spin temperature/covering factor ratio at  $z_{\text{abs}} > 2$  is only double that found at  $z_{\text{abs}} < 2$ . This is significantly lower than the factor of eight in spin temperature, determined from previous estimates of the covering factor.
2. This reduced factor can be accounted for by the effects of an expanding Universe, where the angular diameter distance at  $z_{\text{abs}} > 1$  is always close to, and sometimes exceeds, that of the background radio source. That is, the high redshift DLAs are *always* disadvantaged in how effectively they can intercept the background radio flux for a given DLA–QSO pair.
3. Since the non-detections tend to be associated with high ratios in the DLA–QSO angular diameter distances ( $DA_{\text{abs}}/DA_{\text{QSO}} \approx 1$ ), whereas the detections are associated with low ratios

( $DA_{\text{abs}}/DA_{\text{QSO}} < 1$ ), at *all* redshifts, this strongly suggests that the coverage of the background radio source by the absorber is the dominant factor.

This runs contrary to previous studies which estimate the covering factor via VLBA imaging, which support an evolution in the spin temperature. However, these estimates are based upon several pivotal assumptions, whereas the angular diameter distance ratios are not.

We therefore suggest that there is no evidence for the spin temperature to increase with redshift, which implies no evolution in the fraction of the warm neutral gas content of DLAs. Curran et al. (2007b) find a  $T_{\text{spin}}/f$ –metallicity anti-correlation. If the spin temperature does not evolve with redshift, as does the metallicity (Prochaska et al. 2003; Curran et al. 2004), this may imply that the metallicity is proportional to the covering factor, which could be due to the larger absorbing cross-sections of the larger galaxies, as evident through the spirals which have the largest metallicities and the lower values of  $T_{\text{spin}}/f$  (Curran et al. 2010).

This research has made use of the NASA/IPAC Extragalactic Database (NED) which is operated by the Jet Propulsion Laboratory, California Institute of Technology, under contract with the National Aeronautics and Space Administration. This research has also made use of NASA’s Astrophysics Data System Bibliographic Service and ASURV Rev 1.2 (Lavalley et al. 1992), which implements the methods presented in Isoobe et al. (1986). The Centre for All-sky Astrophysics is an Australian Research Council Centre of Excellence, funded by grant CE11E0090.

#### REFERENCES

- Briggs, F. H. & Wolfe, A. M. 1983, ApJ, 268, 76  
 Curran, S. J. 2010, MNRAS, 402, 2657  
 Curran, S. J., Murphy, M. T., Pihlström, Y. M., Webb, J. K., & Purcell, C. R. 2005, MNRAS, 356, 1509  
 Curran, S. J., Tzanavaris, P., Darling, J. K., Whiting, M. T., Webb, J. K., Bignell, C., Athreya, R., & Murphy, M. T. 2010, MNRAS, 402, 35

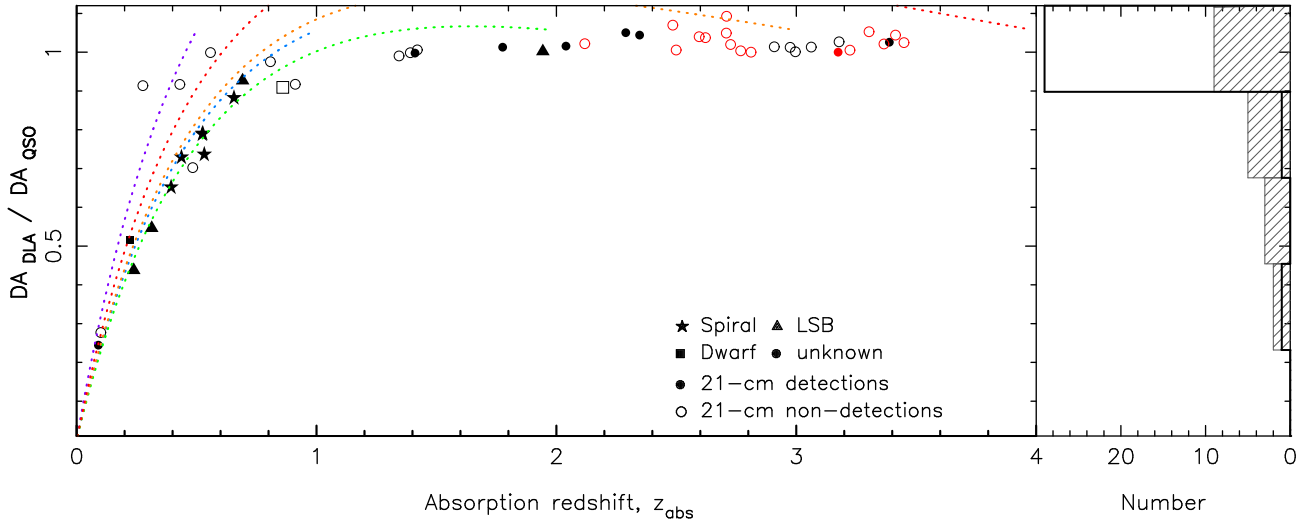


FIG. 4.— The absorber/quasar angular diameter distance ratio versus the absorption redshift for DLAs searched in 21-cm absorption. The symbols and histogram are as per Fig. 2. The iso-redshift curves show how  $DA_{\text{DLA}}/DA_{\text{QSO}}$  varies with absorber redshift, where  $DA_{\text{QSO}}$  is for a given QSO redshift, given by the terminating value of  $z_{\text{abs}}$ . That is, we show  $DA_{\text{DLA}}/DA_{\text{QSO}}$  for  $z_{\text{QSO}} = 0.5, 1, 2, 3$  and 4. We employ a standard  $\Lambda$  cosmology with  $H_0 = 71 \text{ km s}^{-1} \text{ Mpc}^{-1}$ ,  $\Omega_{\text{matter}} = 0.27$  and  $\Omega_{\Lambda} = 0.73$ .

Curran, S. J., Tzanavaris, P., Murphy, M. T., Webb, J. K., & Pihlström, Y. M. 2007a, MNRAS, 381, L6  
 Curran, S. J., Tzanavaris, P., Pihlström, Y. M., & Webb, J. K. 2007b, MNRAS, 382, 1331  
 Curran, S. J. & Webb, J. K. 2006, MNRAS, 371, 356  
 Curran, S. J., Webb, J. K., Murphy, M. T., Bandiera, R., Corbelli, E., & Flambaum, V. V. 2002, PASA, 19, 455  
 Curran, S. J., Webb, J. K., Murphy, M. T., & Carswell, R. F. 2004, MNRAS, 351, L24  
 Curran, S. J., Whiting, M., Murphy, M. T., Webb, J. K., Bignell, C., Polatidis, A. G., Wiklind, T., Francis, P., & Langston, G. 2011a, MNRAS, 413, 1165  
 Curran, S. J. & Whiting, M. T. 2010, ApJ, 712, 303  
 Curran, S. J., Whiting, M. T., Tanna, A., Bignell, C., & Webb, J. K. 2011b, MNRAS, 413, L86  
 Curran, S. J., Whiting, M. T., Webb, J. K., & Athreya, A. 2011c, MNRAS, 414, L26  
 Curran, S. J., Whiting, M. T., Wiklind, T., Webb, J. K., Murphy, M. T., & Purcell, C. R. 2008, MNRAS, 391, 765  
 Hogg, D. W. 1999, astro-ph/9905116  
 Isobe, T., Feigelson, E., & Nelson, P. 1986, ApJ, 306, 490  
 Kanekar, N. & Chengalur, J. N. 2001, A&A, 369, 42  
 —. 2003, A&A, 399, 857

Kanekar, N., Lane, W. M., Momjian, E., Briggs, F. H., & Chengalur, J. N. 2009, MNRAS, 394, L61  
 Lavalley, M. P., Isobe, T., & Feigelson, E. D. 1992, in BAAS, Vol. 24, 839–840  
 Murphy, M. T., Curran, S. J., Webb, J. K., Ménager, H., & Zych, B. J. 2007, MNRAS, 376, 673  
 Noterdaeme, P., Petitjean, P., Ledoux, C., & Srianand, R. 2009, A&A, 505, 1087  
 Prochaska, J. X., Gawiser, E., Wolfe, A. M., Castro, S., & Djorgovski, S. G. 2003, ApJ, 595, L9  
 Prochaska, J. X., Herbert-Fort, S., & Wolfe, A. M. 2005, ApJ, 635, 123  
 Roberts, M. S., Brown, R. L., Brundage, W. D., Rots, A. H., Haynes, M. P., & Wolfe, A. M. 1976, AJ, 81, 293  
 Srianand, R., Gupta, N., Petitjean, P., Noterdaeme, P., Ledoux, C., Salter, C. J., & Saikia, D. J. 2012, MNRAS, accepted (arXiv:1112.1438)  
 Wolfe, A. M. & Burbidge, G. R. 1975, ApJ, 200, 548  
 Wolfe, A. M., Gawiser, E., & Prochaska, J. X. 2005, ARA&A, 43, 861